Differences in quasielastic cross sections of muon and electron neutrinos

Melanie Day and Kevin S. McFarland

Phys. Rev. D **86**, 053003 — Published 11 September 2012

DOI: 10.1103/PhysRevD.86.053003

Differences in Quasi-Elastic Cross-Sections of Muon and Electron Neutrinos

Melanie Day
University of Rochester, Department of Physics and Astronomy, Rochester, NY 14627 USA

Kevin S. McFarland
University of Rochester, Department of Physics and Astronomy, Rochester, NY 14627 USA
and Fermi National Accelerator Laboratory, Batavia, IL 60510 USA

(Dated: August 10, 2012)

Accelerator neutrino oscillation experiments seek to make precision measurements of the neutrino flavor oscillations $\overset{(-)}{\nu}_\mu \to \overset{(-)}{\nu}_e$ in order to determine the mass hierarchy of neutrinos and to search for CP violation in neutrino oscillations. These experiments are currently performed with beams of muon neutrinos at energies near 1 GeV where the charged-current quasi-elastic interactions $\nu_\ell n \to \ell^- p$ and $\bar{\nu}_\ell p \to \ell^+ n$ dominate the signal reactions. We examine the difference between the quasi-elastic cross-sections for muon and electron neutrinos and anti-neutrinos and estimate the uncertainties on these differences.

I. INTRODUCTION

Since the invention of neutrino beams at accelerators and the consequent discovery of the two flavors of neutrinos[1], the reactions $\nu_\ell n \to \ell^- p$ and $\bar{\nu}_\ell p \to \ell^+ n$, which are the dominant reactions of muon and electron neutrinos with energies from 200 MeV to 2 GeV, have played an important role in studies of neutrino flavor. These charged-current quasi-elastic (CCQE) interactions are important not only because they identify the flavor of the neutrino through the production of the lepton in the final state, but also because the two body kinematics permit a measurement of the neutrino energy from only the observation of the final state lepton.

Accelerator neutrino experiments like T2K[2, 3], NOvA[4] and a number of proposed experiments seek to make precision measurements of the neutrino flavor oscillations $\overset{(-)}{\nu}_\mu \to \overset{(-)}{\nu}_e$ or $\overset{(-)}{\nu}_e \to \overset{(-)}{\nu}_\mu$ in order to determine the mass hierarchy of neutrinos and to search for CP violation in neutrino oscillations. Uncertainties on differences between these cross-sections for muon and electron neutrinos will contribute to experimental uncertainties in these flavor oscillation measurements.

Interactions of the charged-current with fundamental fermions, such as $\nu_\ell d \to \ell^- u$, have no uncertainties in the differences between the reactions for muon and electron neutrino interactions because the weak interaction is experimentally observed to be flavor universal. In particular, the effect of the final state lepton mass in this two body reaction of fundamental fermions can be unambiguously calculated.

One such calculable difference occurs because of radiative corrections to the tree-level CCQE process. Radiative corrections from a particle of mass m in a process with momentum transfer Q are of order $\frac{\alpha}{\pi}\log\frac{Q}{m}$, which implies a significant difference due to the mass of the final state lepton[5]. Although this effect is calculable, it is not accounted for in neutrino interaction generators used in recent analysis of experimental data, such as GENIE[6], NEUT[7, 8] and NUANCE[9].

There are, however, cross-section differences due to lepton mass which cannot be calculated from first principles with current theoretical tools. The presence of the target quarks inside a strongly bound nucleon lead to a series of *a priori* unknown form factors in the nucleon level description of the reaction, e.g., $\nu_\ell n \to \ell^- p$. It is the uncertainties on these form factors combined with the alteration of the kinematics due to lepton mass that leads to uncertainties, and that is the focus of the results of this paper.

There is also a modification of the reaction cross-sections due to the effects of the nucleus in which the target nucleons are bound. The model incorporated in GENIE[6], NEUT[7, 8] and NUANCE[9] is a relativistic Fermi gas model[10, 11] which provides a distribution of nucleon kinematics inside the nucleus. A more sophisticated description from a nuclear spectral function model[12] is implemented in the NuWro generator[13]. Each of these models build upon the free nucleon CCQE cross-section as an input. We do not consider the effect of the nucleus in this work, although it may be important in the relative weighting of nucleon kinematics at low energy and low Q^2. However, by specifying possible modifications to the assumed free nucleon cross-section, this work provides a blueprint for studying the effect of the final state lepton mass in different nuclear models.

II. NUCLEON FORM FACTORS

The cross section for quasi-elastic scattering of neutrinos at energies relevant for oscillation experiments may be calculated from the Fermi theory of weak interactions with the effective Lagrangian,

$$\mathcal{L}_{\text{eff}} = \frac{G_F}{\sqrt{2}}\left(J^\dagger_{(\ell)\lambda} J^\lambda_{(H)} + \text{Hermitian conjugate}\right), \quad (1)$$

where G_F is the Fermi constant and the J are the leptonic and hadronic currents. The form of the leptonic current

is specified by the theory to be

$$J_{(\ell)\lambda} = \bar{\psi}_\ell \gamma_\lambda (1-\gamma_5)\psi_{\nu_\ell}, \tag{2}$$

because the leptons are fundamental fermions. However, as mentioned above the hadronic current for quasi-elastic scattering depends on unknown form factors of the nucleons. The hadronic current can be decomposed into vector and axial components,

$$J^\lambda_{(H)} = J^\lambda_V + J^\lambda_A. \tag{3}$$

J_V contains three terms related to the vector form factors F_V^1, F_V^2 and F_V^3, and J_A contains three terms related to the axial form factors F_A, F_A^3 and F_p. A description the the bilinear covariant structure of the currents is given in several standard texts and review papers[14–16]. We follow most closely the notation of Ref. 15.

From the effective Lagrangian of Eq. 1 and currents above in Eqs. 2 and 3, the quasi-elastic cross section on free nucleons is:

$$\frac{d\sigma}{dQ^2}(^{\nu n\to l^- p}_{\overline{\nu} p\to l^+ n}) = \left[A(Q^2) \mp B(Q^2)\frac{s-u}{M^2} + C(Q^2)\frac{(s-u)^2}{M^4}\right] \times \frac{M^2 G_F^2 \cos^2\theta_c}{8\pi E_\nu^2} \tag{4}$$

where the invariant $Q^2 = -q^2$ and q is the four momentum transfer from the leptonic to hadronic system, M is the mass of the nucleon, θ_c is the Cabibbo angle, and E_ν is the neutrino energy in the lab. The combination of Mandelstam invariants s and u can be written as,

$$s - u = 4ME_\nu - Q^2 - m^2, \tag{5}$$

where m is the mass of the final state lepton. The functions A(Q^2), B(Q^2) and C(Q^2) depend on the nucleon form factors and ξ, the difference between the anomalous magnetic moment of the proton and the neutron:

$$A(Q^2) = \frac{m^2+Q^2}{4M^2}\left[\left(4+\frac{Q^2}{M^2}\right)|F_A|^2 - \left(4-\frac{Q^2}{M^2}\right)|F_V^1|^2 + \frac{Q^2}{M^2}\xi|F_V^2|^2\left(1-\frac{Q^2}{4M^2}\right) + \frac{4Q^2 Re F_V^{1*}\xi F_V^2}{M^2} - \frac{Q^2}{M^2}\left(4+\frac{Q^2}{M^2}\right)|F_A^3|^2 - \frac{m^2}{M^2}\left(|F_V^1+\xi F_V^2|^2 + |F_A+2F_P|^2 - \left(4+\frac{Q^2}{M^2}\right)\left(|F_V^3|^2+|F_P|^2\right)\right)\right], \tag{6}$$

$$B(Q^2) = \frac{Q^2}{M^2} Re F_A^*\left(F_V^1+\xi F_V^2\right) - \frac{m^2}{M^2} Re\left[\left(F_V^1 - \frac{Q^2}{4M^2}\xi F_V^2\right)^* F_V^3 - \left(F_A - \frac{Q^2 F_P}{2M^2}\right)^* F_A^3\right] \text{ and} \tag{7}$$

$$C(Q^2) = \frac{1}{4}\left(|F_A|^2 + |F_V^1|^2 + \frac{Q^2}{M^2}\left|\frac{\xi F_V^2}{2}\right|^2 + \frac{Q^2}{M^2}|F_A^3|^2\right). \tag{8}$$

Note that the form factors themselves are functions of Q^2 in Eqs. 6–8.

F_V^1 and F_V^2 are the vector and F_A and F_P the axial form factors of the first class currents. First class currents conserve both time and charge symmetry. In addition, first class vector currents commute with the G-parity operator while first class axial currents anti-commute with it[14]. The terms associated with F_V^1 and F_A are considered the leading terms in the hadron current since they have no dependence on the four-momentum transfer, excepting that of the form factors, and they are not suppressed by powers of the final state lepton mass as F_P is.

Vector elastic form factors are precisely known at $Q^2 = 0$ from the nucleon electric charges and magnetic moments and are precisely measured over a wide range of Q^2 in charged-lepton elastic scattering from protons and deuterium. The axial nucleon form factor at zero Q^2 is precisely measured in studies of neutron beta decay. At higher Q^2, much of our knowledge of the axial form factors comes from muon neutrino quasi-elastic scattering measurements. For $Q^2 \lesssim 1$ (GeV/c)^2, the vector form factors and the axial form factors are observed to follow a dipole form, that is

$$F(Q^2) \propto F(0)/(1+Q^2/C^2)^2 \tag{9}$$

where the constant C is often expressed as a mass of the same order of magnitude as the mass of the nucleon. At high Q^2 the vector form factors do not follow the dipole structure[18]. The neutrino scattering data contains conflicting results among different experiments[19–23] which limit our ability to effectively use that information to constrain the axial form factor. Pion electroproduction experiments[24, 25] have also measured the axial form factor at $Q^2 < 0.2$ (GeV/c)^2.

The form factor F_P is determined from PCAC which, under minimal assumptions, states that[26]:

$$\delta_\mu J_A^\mu = C\phi \tag{10}$$

where ϕ is the renormalized field operator that creates the π^+ and C is a constant which may be computed at $Q^2 = 0$. PCAC gives the following relation between F_P

and the pion nucleon form factor, $g_{\pi NN}$,

$$F_P(Q^2) = \frac{2M^2 F_A(0)}{Q^2} \times \left(\frac{F_A(Q^2)}{F_A(0)} - \frac{g_{\pi NN}(Q^2)}{g_{\pi NN}(0)} \frac{1}{(1+\frac{Q^2}{M_\pi^2})} \right), \quad (11)$$

where M_π is the pion mass. The Goldberger-Treiman relation[27] predicts

$$g_{\pi NN}(Q^2) F_\pi = F_A(Q^2) M, \quad (12)$$

where F_π is the pion decay constant. Under the assumption that the Goldberger-Treiman relation holds for all values of Q^2, then F_P is

$$F_P(Q^2) = \frac{2M^2 F_A(Q^2)}{M_\pi^2 + Q^2}. \quad (13)$$

This is the relationship that is used in all modern neutrino generators[6–9, 13].

F_V^3 and F_A^3 are form factors associated with the second class current (SCC). The existence of such currents requires charge or time symmetry violation, and current measurements show the size of these violations to be small. Additionally a nonzero F_V^3 term would violate conservation of the vector current (CVC). Both $F_V^3(0)$ and $F_A^3(0)$ can be limited experimentally in studies of beta decay. Almost all current analyses of neutrino data assume that the SCCs are zero. The vector SCCs only enter the cross-section in terms suppressed by m^2/M^2, but there are unsuppressed terms involving the axial SCC form factor.

III. MUON AND ELECTRON NEUTRINO QUASI-ELASTIC CROSS SECTION DIFFERENCES

In this section, we will study the dependence of the muon-electron cross-section differences as a function of E_ν and Q^2. Differences arise due to the variation of kinematic limits due to the final state lepton mass, different radiative corrections to the tree level process and uncertainties in nucleon form factors. Equations 6 and 7 contain explicitly the dependence of the CCQE cross-section in terms of the form factors. Lepton mass, m, enters in both $A(Q^2)$ and $B(Q^2)$ and these terms involve all the form factors discussed above. Note that F_P and F_V^3 *only* appear in terms multiplied by m^2/M^2 and therefore are negligible in the electron neutrino cross-section, but not in the muon neutrino cross-section.

As metrics, we define the fractional differences between the muon and electron neutrino CCQE cross-sections:

$$\delta(E_\nu, Q^2) \equiv \frac{\frac{d\sigma_\mu}{dQ^2} - \frac{d\sigma_e}{dQ^2}}{\int dQ^2 \frac{d\sigma_e}{dQ^2}} \quad (14)$$

$$\Delta(E_\nu) \equiv \frac{\int dQ^2 \frac{d\sigma_\mu}{dQ^2} - \int dQ^2 \frac{d\sigma_e}{dQ^2}}{\int dQ^2 \frac{d\sigma_e}{dQ^2}}. \quad (15)$$

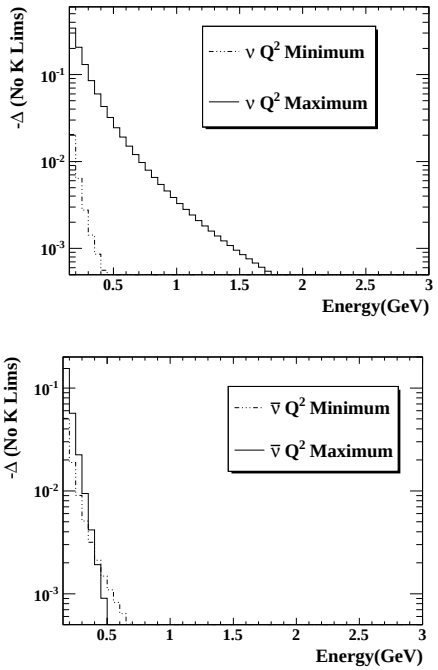

FIG. 1. The total charged-current quasi-elastic cross-section difference for neutrinos (top) and anti-neutrinos (bottom) due to the kinematic limits in Q^2. This difference is $-\Delta$ defined in Eq. 15, meaning that the electron neutrino cross-section is larger than the muon neutrino cross-section.

The integrals over Q^2 in Eqs. 14 and 15 are taken within the kinematic limits of each process, and those limits depend on lepton mass as discussed in the next section.

Another useful metric is the difference between a cross-section in a model with a varied assumption from that of a reference model. Our reference model derives F_V^1 and F_V^2 from the electric and magnetic vector Sachs form factors which follow the dipole form of Eq. 9 with $C = c^2 M_V^2 = (0.84)$ (GeV/c)^2, and it assumes F_A is a dipole with $C = c^2 M_A^2 = (1.1)$ (GeV/c)^2. The reference model uses the derived F_P from Eq. 13, and assumes that $F_V^3 = F_A^3 = 0$ at all Q^2. We then define:

$$\Delta_\ell(E\nu) \equiv \frac{\int dQ^2 \frac{d\sigma_\ell}{dQ^2} - \int dQ^2 \frac{d\sigma_\ell^{ref}}{dQ^2}}{\int dQ^2 \frac{d\sigma_\ell^{ref}}{dQ^2}}, \quad (16)$$

where σ_ℓ^{ref} is the reference model for $\nu_\ell n \to \ell^- p$ or its anti-neutrino analogue and σ_ℓ is the model to be compared to the reference.

A. Kinematic Limits

The neutrino and anti-neutrino CCQE processes have kinematic limits in Q^2 which depend on the final state lepton mass, m. These limits are

$$Q^2_{\substack{max \\ min}} = -m^2 + \frac{s - M^2}{\sqrt{s}} \left(E_\ell^* \pm |p_\ell^*| \right) \quad (17)$$

where s is the Mandelstam invariant representing total center of mass energy and E_ℓ^* and p_ℓ^* are the center of

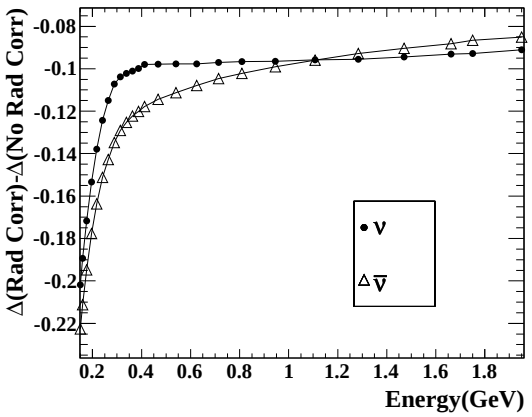

FIG. 2. Our estimate in the lepton leg leading log approximation of the fractional difference between the electron and muon neutrino total charged-current quasi-elastic cross-sections, Δ as defined in Eq. 15, as a function of neutrino energy. The negative difference means that the electron neutrino cross-section is larger than the muon neutrino cross-section.

mass final state lepton energy and momentum. E_ℓ^* can be expressed in terms of invariants as

$$E_\ell^* = \frac{s + m^2 - M^2}{2\sqrt{s}}. \tag{18}$$

Figure 1 shows the effect of the kinematic limits. Not surprisingly, the effect is very large near the threshold for the muon neutrino and anti-neutrino reaction. These effects are accounted for in the description of the quasi-elastic process in all commonly used neutrino generators. However, it is worth noting that the difference in Q^2 spanned by the two reactions can lead to large effects in varying form factors that significantly affect either the small or large Q^2 parts of the cross-section.

B. Radiative Corrections

To calculate the effect of radiative corrections on the total quasi-elastic cross-section, we follow the approximate approach of calculating the leading log correction to order $\log Q/m$, where Q is the energy scale of the interaction process[5]. This approach has a calculational advantage in investigating the differences due to the lepton mass, m because the lepton leg leading log only involves sub-processes where photons attach to leptons. The key result from this approach is that the cross-section which allows for the presence of radiated photons, σ_{LLL} is related to the Born level cross-section, σ_B, by

$$\frac{d\sigma_{LLL}}{dE_\ell d\Omega} \approx \frac{d\sigma_B}{dE_\ell d\Omega} + \frac{\alpha_{EM}}{2\pi}\log\frac{4E_\ell^*}{m^2}\int_0^1 dz \frac{1+z^2}{1-z} \times \left(\frac{1}{z}\frac{d\sigma_B}{d\hat{E}_\ell d\Omega}\Big|_{\hat{E}_\ell = E_\ell/z} - \frac{d\sigma_B}{dE_\ell d\Omega}\right), \tag{19}$$

where E_ℓ^* is the center-of-mass frame lepton energy.

In the case of elastic scattering, the relationship in σ_B between E_ℓ and the scattering angle, θ_ℓ simplifies the calculation because there is at most one z in the integrand for which the cross-section does not vanish for a particular lepton angle:

$$z = \left[2E_\ell\left(M + E_\nu\right)\left(m^2 + 2ME_\nu\right) - 2\cos^2\theta_\ell E_\ell E_\nu \times \sqrt{m^4 + 4E_\nu^2\left(M^2 - m^2\sin^2\theta_\ell\right) - 4m^2M^2 - 4m^2ME_\nu}\right] / \left[m^4 + 4E_\nu\left(E_\nu\left(m^2\cos^2\theta_\ell + M^2\right) + m^2M\right)\right]. \tag{20}$$

We then obtain the remaining cross-section by integrating Eq. 19 over the final state lepton energy. Note that this procedure only gives a prescription for evaluating $d\sigma(E_{\nu,true})/dQ^2_{true}$; however, the radiation of real photons means that the relationship between lepton energy and angle and E_ν and Q^2 in elastic scattering will no longer be valid. The effect of this distortion of the elastic kinematics will depend on the details of the experimental reconstruction and the neutrino flux seen by the experiment, so the effect must be evaluated in the context of a neutrino interaction generator and full simulation of the reconstruction for a given experiment.

The difference of the effect on the total cross-sections as a function of neutrino energy is shown in Fig. 2. We estimate a difference of approximately 10% over the energies of interest in oscillation experiments. The largest differences fractional differences in cross-sections are at high true Q^2 and low neutrino energies. The magnitude of the lepton leg correction to the muon neutrino total cross-section is smaller, roughly 0.4 times this difference, so the larger effect is on the electron neutrino cross-section.

Our estimation of the effect is surprisingly large at the relevant energies for oscillation experiments. Some portion of this difference in the total cross-section in Fig. 2 may be canceled by diagrams missing from the leading log correction in the lepton leg, such as box diagrams involving $W\gamma$ exchange between the leptonic legs and the initial or final state, which will also depend on the final state lepton mass [17]. We stress that this is only an approximate treatment which should be confirmed in a full calculation implemented inside a generator, and to date radiative corrections are not included in the commonly used neutrino interaction generators[6–9].

C. Uncertainties in F_V^1, F_V^2 and F_A

As noted above, the vector form factors F_V^1 and F_V^2 are precisely measured in charged lepton scattering[18]; however, the axial form factor is still uncertain because neutrino experiments that measure it do not agree amongst themselves or with determinations in pion electroproduction as discussed above. Therefore the axial form factor will dominate any differences in the electron and muon

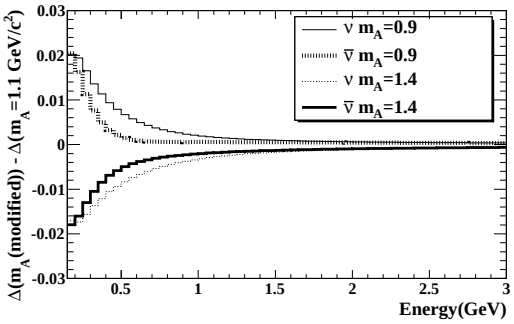

FIG. 3. The change in the fractional difference of muon CCQE cross-section and electron CCQE when m_A is changed from a reference value of 1.1 GeV/c^2 in a range generously consistent with current experimental data.

cross-sections due to uncertainties in leading form factors.

Figure 3 illustrates the change in the fractional difference of muon and electron neutrino CCQE cross-sections when the axial form factor is varied by changing the assumed dipole mass in a range consistent with experimental measurements. The size of the effect is of order 1% at very low energy and drops with increasing energy. This difference in cross-section may be accounted for in variations of the axial form factor within the analysis of an experiment using a modern neutrino interaction generator.

D. Pseudoscalar Form Factor

At low Q^2, the pseudoscalar form factor does have a significant contribution to the muon neutrino CCQE cross-section, of nearly the same order of the leading terms. However, Eq. 13 shows that the contribution will be suppressed for $Q^2 \gtrsim M_\pi^2$, and all terms involving F_P are suppressed by m/M and so the contribution to the cross-section is negligible for electron neutrinos. At low neutrino energies, the pseudoscalar form factor effect on the cross-section difference, $\Delta(E_\nu)$ is nearly as large as that of the kinematic limits. The effect of the form factor as a function of neutrino energy and Q^2 is different for neutrinos and anti-neutrinos.

Current neutrino interaction generators[6–9] include the effect of F_P shown in Eq. 13 under the assumptions of PCAC and that the Goldberger-Treiman relation holds for all Q^2. Experimental tests of the Goldberger-Treiman relation have identified small discrepancies which imply that the left hand side of Eq. 12 is between 1% and 6% less than the right-hand side[28, 29]. Guidance from models suggests that this effect is likely to disappear at high Q^2[30]. We examine the effect of varying $F_P(0)$ by 3% of itself as a reasonable approximation to the possible difference due to this effect. A more significant difference may arise due to violations of PCAC. This has been directly checked in pion electroproduction studies[24] which can directly measure $F_P(Q^2)$ in the range of 0.05 to 0.2 GeV/c^2. Uncertainties in this data limit the reasonable range of pole masses in Eq. 11 to be between $0.6M_\pi$ and $1.5M_\pi$. Effects due to these possible deviations from PCAC and the Goldberger-Treiman relation are shown in Fig. 4 along with the effect of assuming $F_P = 0$ for comparison.

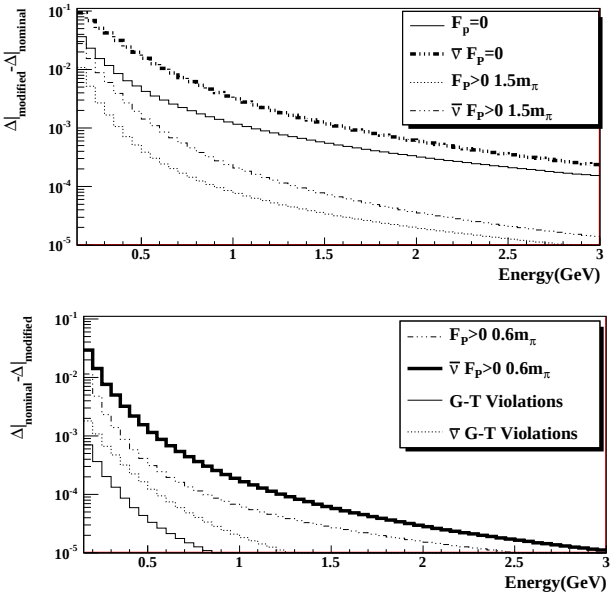

FIG. 4. The effect of variations of F_P from the reference model which assumes PCAC and the Goldberger-Treiman relation. The plots illustrate the change cross-section difference, $\Delta(E_\nu)$, between a varied model and the reference model. Possible violations of the G-T relation produce a negligibly small effect, even at low energy. The range of violations from PCAC allowed by current data would allow significantly larger changes. The effect of setting F_P to zero is shown for comparison.

E. Second Class Currents

As noted in the introductory material, non-zero second class currents violate a number of symmetries and hypotheses, and are therefore normally assumed to be zero in analysis of neutrino reaction data and in neutrino interaction generators. For this study, we take a data driven approach and look at the effect of the largest possible second-class current form factors, F_V^3 and F_A^3 that do not violate constraints from this data.

Vector second-class currents enter the cross-sections for neutrino quasi-elastic scattering always suppressed by m/M and therefore only appear practically in muon neutrino scattering cross-sections. Both vector and axial vector form factors give large contributions to the $B(Q^2)$ term given in Eqs. 4 and 7, and therefore typically have very different effects, often even different in sign, for neutrino and anti-neutrino scattering.

The vector second-class currents are difficult to detect in most weak processes involving electrons because

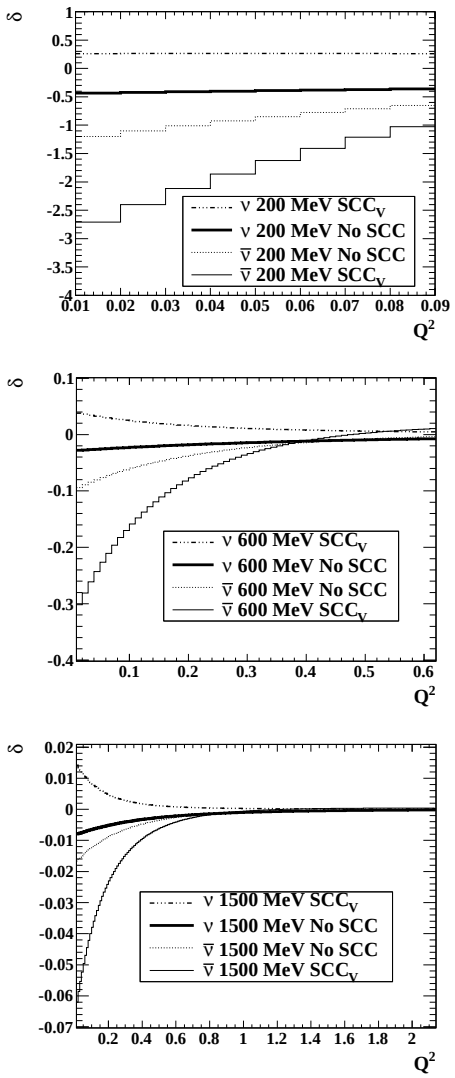

FIG. 5. $\delta(E_\nu, Q^2)$, defined in Eq. 14, as a function of Q^2 for several selected E_ν. The difference between including and not including the maximum allowed second class vector current ("SCC$_V$"), $F_V^3(Q^2) = 4.4F_V^1(Q^2)$, is shown.

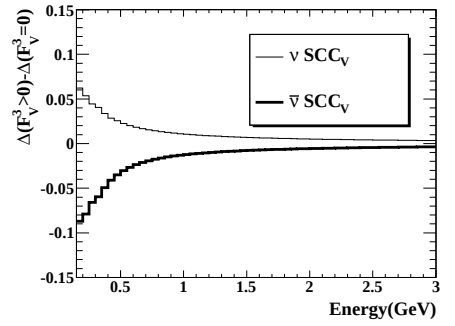

FIG. 6. Changes in the difference between the muon and electron neutrino cross sections due to including F_V^3.

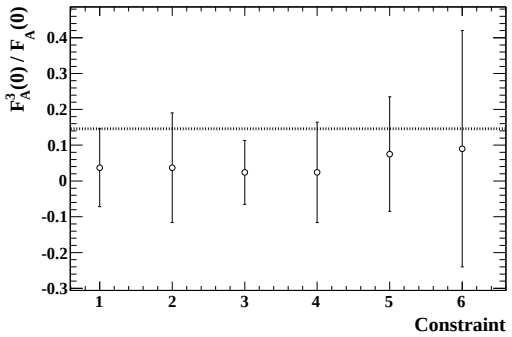

FIG. 7. A survey of constraints on the ratio $F_A^3(0)/F_A(0)$ with their uncertainties from: (1) Wilkinson's data compilation[38], (2) the same Wilkinson compilation with a correction for short-range effects[38], (3) the method of Wilkinson applied only to the $A = 20$ KDR parameters[37, 38], (4) ibid, with a correction for short-range effects[37, 38], (5) a derived limit from $A = 12$ beta decays[36] and (6) a derived limit from $A = 20$ beta decays[37]. The value used for $F_A^3(0)/F_A(0)$ in this study is shown by the dashed line.

the process is generally suppressed by powers of m_e/M. Therefore even very precise beta decay measurements have difficulty limiting the size of $F_V^3(0)$ to less than several times the magnitude of the regular vector form factors[31]. The best limits from beta decays currently limit $F_V^3(0)/F_V^1(0)$ to be $(0.0011 \pm 0.0013)\frac{m_N}{m_e} \approx 2.0 \pm 2.4$[32]. Studies of muon capture on nuclei can provide modestly better limits, but at the expense of assuming there are no axial second class currents[31]. An analysis of anti-muon neutrino quasi-elastic scattering has been used to place limits of similar strength, but again under the assumption of no axial second class currents and with an assumed Q^2 dependence, $F_V^3(Q^2) = F_V^3(0)/(Q^2 + M_{3V}^2)^2$ with a fixed M_{3V} of 1.0 GeV/c^2[33]. From the preponderance of the data, we choose to parameterize the maximum size of the allowed vector second class current as $F_V^3(Q^2) = 4.4F_V^1(Q^2)$, which is not excluded by the results of any of the above studies. The effect of this is significant, particularly at low neutrino energies and is shown in Figs. 5 and 6. Recall that the effect on the electron neutrino cross-section from F_V^3 is negligible, so this effect occurs almost entirely in the muon neutrino cross-section.

By contrast, the axial second class current at zero Q^2 is reasonably well constrained by studies of beta decay. We derive our limits in the framework of the KDR parameters[34] where there is a wealth of experimental data to constrain these parameters[35–38] and therefore derive a limit on $F_A^3(0)$. Figure 7 shows these experimental constraints and the effect we allow in this study.

We assume a dipole form for the variation in Q^2 of the axial second class current as well, so that for the maximum allowed variation $F_A^3(Q^2)/F_A(Q^2) = F_A^3(0)/F_A(0) = 0.15$. Figure 8 shows the effect of including this allowed axial second class current on both the difference of electron and muon neutrino cross-sections and on the muon neutrino cross-section itself. It is signif-

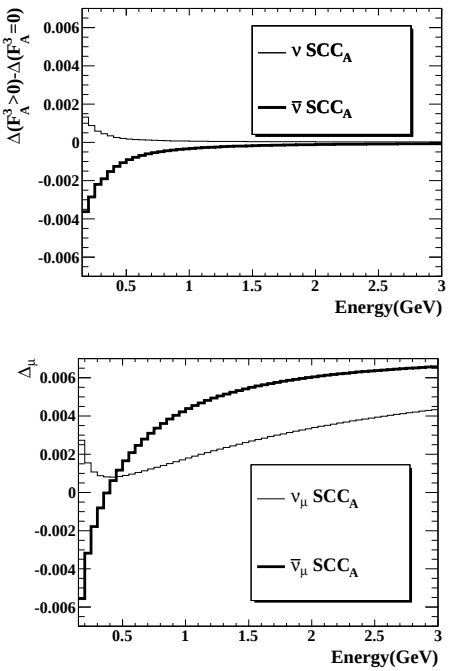

FIG. 8. Top: Changes in the difference between the muon and electron neutrino cross sections due to including F_A^3; Bottom: the change in muon neutrino cross-sections due to including F_A^3.

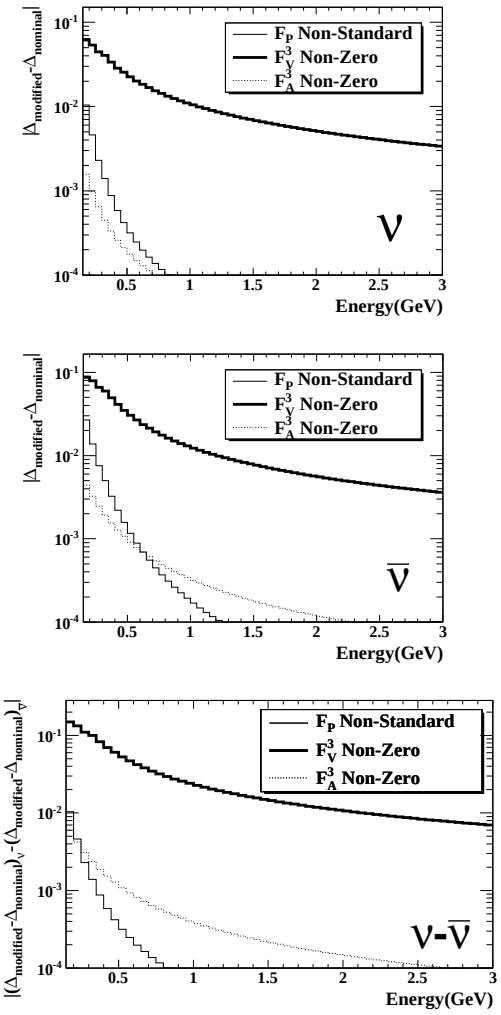

FIG. 9. Top and Middle: For the form factors not well constrained and not accounted for in neutrino generators, a summary of the magnitude of the fractional size of differences in the total charged-current quasi-elastic cross-sections between electron and muon neutrinos and anti-neutrinos as a function of neutrino energy. For F_P the average of the magnitude of the PCAC violating effects are summed linearly with the magnitude of the Goldberger-Treiman violation effect. Bottom: The magnitude of the difference between ν and $\bar{\nu}$ of the fractional differences which illustrates the size of apparent CP violating asymmetries in oscillation experiments.

icantly smaller than the effect of the vector second class current because the limits on these currents are more stringent.

IV. CONCLUSIONS

Large differences between the electron and muon neutrino quasi-elastic cross-sections exist at low neutrino energies from the presence of different kinematic limits due to the final state lepton mass and due to the presence of the pseudoscalar form factor, F_P, derived from PCAC and the Goldberger-Treiman relation. These differences are typically accounted for in modern neutrino interaction generators.

There are also significant differences due to radiative corrections, particularly in diagrams that involve photon radiation attached to the outgoing lepton leg which are proportional to $\log Q/m$. These differences are calculable, but are typically not included in neutrino interaction generators employed by neutrino oscillation experiments. If our estimate of these differences, of order 10%, is confirmed by more complete analyses, then this is a correction that needs to be included as it is comparable to the size of current systematic uncertainties at accelerator experiments[2, 3].

Modifications of the assumed F_P from PCAC and the Goldberger-Treiman relation and the effect of the form factors F_V^3 and F_A^3 corresponding to second class vector and axial currents, respectively, are not included in neutrino interaction generators. A summary of the possible size of these effects, as we have estimated them, is shown in Fig. 9.

These differences, particularly from the second class vector currents, may be significant for current[2–4] and future[39] neutrino oscillation experiments which seek precision measurements of $\nu_\mu \to \nu_e$ and its anti-neutrino counterpart at low neutrino energies. Previous work[33] has demonstrated sensitivity to these second class currents in neutrino and anti-neutrino quasi-elastic muon

neutrino scattering, and future work with more recent data[20, 23] and newly analyzed data[40] may help to further limit uncertainties on possible second class currents.

ACKNOWLEDGMENTS

The suggestion for this work came out of conversations with Alain Blondel about systematics in future oscillation experiments and we thank him for inspiring this work. We are grateful to Ashok Das, Tamar Friedmann and Tom McElmurry for their clear and patient explanations of the bilinear covariant structure of weak interactions. We thank Arie Bodek for a helpful discussion of available tests of the CVC hypothesis. We thank Gabriel Perdue and Geralyn Zeller for helpful comments on a draft of this manuscript. We are grateful to Bill Marciano for his helpful insights into the radiative corrections after the initial draft of this paper appeared online.

This material is based upon work supported by the Department of Energy under Award Number DE-FG02-91ER40685.

[1] G. Danby *et al.*, Phys. Rev. Lett. **9**, 36–44 (1962).
[2] Y. Itow *et al.* [The T2K Collaboration], hep-ex/0106019.
[3] K. Abe *et al.* [T2K Collaboration], Phys. Rev. Lett. **107**, 041801 (2011).
[4] D. Ayres *et al.* [NOvA Collaboration], hep-ex/0503053 (2004).
[5] A. De Rujula, R. Petronzio and A. Savoy-Navarro, Nucl. Phys. B **154**, 394 (1979).
[6] C. Andreopoulos [GENIE Collaboration], Acta Phys. Polon. B **40**, 2461 (2009).
[7] Y. Hayato, Nucl. Phys. Proc. Suppl. **112**, 171 (2002).
[8] Y. Hayato, Acta Phys. Polon. B **40**, 2477 (2009).
[9] D. Casper, Nucl. Phys. Proc. Suppl. **112**, 161 (2002).
[10] R.A. Smith and E.J. Moniz Nucl. Phys. **B43** 605 (1972).
[11] A. Bodek and J.L. Ritchie, Phys. Rev. **D23** 1070 (1981).
[12] O. Benhar, A. Fabrocini, S. Fantoni and I. Sick, Nucl. Phys. A **579**, 493 (1994).
[13] J. Sobczyk, PoS NUFACT **08**, 141 (2008).
[14] R.E Marshak, Riazuddin and C.P. Ryan, *Theory of Weak Interactions in Particle Physics*, Wiley-Interscience (1969).
[15] C.H. Llewellyn-Smith, PhysṘept. **3C**, 261–379 (1972).
[16] D.H. Wilkinson, Nucl. Inst. & Meth. **A455**, 656–659 (2000).
[17] A. Sirlin and W. J. Marciano, Nucl. Phys. B **189**, 442 (1981).
[18] A. Bodek, S. Avvakumov, R. Bradford and H. Budd, Eur. Phys. J. **C53**, 349–354 (2008).
[19] A. Bodek, S. Avvakumov, R. Bradford and H. S. Budd, J. Phys. Conf. Ser. **110**, 082004 (2008).
[20] V. Lyubushkin *et al.* [NOMAD Collaboration], Eur. Phys. J. C **63**, 355 (2009).
[21] J. L. Alcaraz-Aunion *et al.* [SciBooNE Collaboration], AIP Conf. Proc. **1189**, 145 (2009).
[22] M. Dorman [MINOS Collaboration], AIP Conf. Proc. **1189**, 133 (2009).
[23] A. A. Aguilar-Arevalo *et al.* [MiniBooNE Collaboration], Phys. Rev. D **81**, 092005 (2010).
[24] S. Choi, V. Estenne, G. Bardin, N. De Botton, G. Fournier, P. A. M. Guichon, C. Marchand and J. Marroncle *et al.*, Phys. Rev. Lett. **71**, 3927 (1993).
[25] A. Liesenfeld *et al.* [A1 Collaboration], Phys. Lett. B **468**, 20 (1999).
[26] Stephen L. Adler, Phys. Rev. **137**, 1022–1033 (1964).
[27] M. L. Goldberger and S. B.Treiman, Phys. Rev. **5**, 1178-1184 (1958).
[28] Thomas Becher and Heinrich Leutwyler, JHEP **6**, 17-34 (2001).
[29] José L. Goitya, Randy Lewisa, Martin Schvellingera and Longzhe Zhanga, Phys. Lett. **B454**, 115122 (1999).
[30] C. Alexandrou, G. Koutsou, Th. Leontiou, J.W. Negele and A. Tsapalis, Phys. Rev. **D76**, 094511 (2007).
[31] B. R. Holstein, Phys. Rev. C **29**, 623 (1984).
[32] J. C. Hardy and I. S. Towner, Phys. Rev. C **71**, 055501 (2005) [nucl-th/0412056].
[33] L. A. Ahrens *et al.*, Phys. Lett. B **202**, 284 (1988).
[34] K. Kubodera, J. Delorme and M. Rho, Nucl. Phys. **B66**, 253-292 (1973).
[35] M. Oka and K. Kubodera, Phys. Lett. **B90** 45 (1980).
[36] K. Minamisono *et al.*, Phys. Rev. **C65**, 015501 (2001).
[37] K. Minamisono *et al.*, Phys. Rev. **C84**, 055501 (2011).
[38] D.H. Wilkinson, Eur. Phys. J. **A7** 307 (2000).
[39] T. Akiri *et al.* [LBNE Collaboration], arXiv:1110.6249 [hep-ex].
[40] K. S. McFarland [The MINERvA Collaboration], AIP Conf. Proc. **1405**, 95 (2011) [arXiv:1108.0702 [hep-ex]].